BIOCHEMISTRY
including biophysical chemistry & molecular biology
Article

Biochemistry **2009,** *48,* 10693–10704 10693
DOI: 10.1021/bi9003815

Synthesis and Evaluation of a Novel Class of G-Quadruplex-Stabilizing Small Molecules Based on the 1,3-Phenylene-Bis(piperazinyl benzimidazole) System†

Akash K. Jain,‡ Vishnu Vardhan Reddy,§ Ananya Paul,‡ K. Muniyappa,§ and Santanu Bhattacharya*,‡,∥

‡*Department of Organic Chemistry, Indian Institute of Science, Bangalore 560012, India,* §*Department of Biochemistry, Indian Institute of Science, Bangalore 560012, India, and* ∥*Chemical Biology Unit, Jawaharlal Nehru Centre for Advanced Scientific Research, Bangalore 560012, India*

Received March 6, 2009; Revised Manuscript Received August 31, 2009

ABSTRACT: Achieving stabilization of telomeric DNA in G-quadruplex conformation by various organic compounds has been an important goal for the medicinal chemists seeking to develop new anticancer agents. Several compounds are known to stabilize G-quadruplexes. However, relatively few are known to induce their formation and/or alter the topology of the preformed quadruplex DNA. Herein, four compounds having the 1,3-phenylene-bis(piperazinyl benzimidazole) unit as a basic skeleton have been synthesized, and their interactions with the 24-mer telomeric DNA sequences from *Tetrahymena thermophilia* $d(T_2G_4)_4$ have been investigated using high-resolution techniques such as circular dichroism (CD) spectropolarimetry, CD melting, emission spectroscopy, and polyacrylamide gel electrophoresis. The data obtained, in the presence of one of three ions (Li^+, Na^+, or K^+), indicate that all the new compounds have a high affinity for G-quadruplex DNA, and the strength of the binding with G-quadruplex depends on (i) phenyl ring substitution, (ii) the piperazinyl side chain, and (iii) the type of monovalent cation present in the buffer. Results further suggest that these compounds are able to abet the conversion of the intramolecular quadruplex into parallel stranded intermolecular G-quadruplex DNA. Notably, these compounds are also capable of inducing and stabilizing the parallel stranded quadruplex from randomly structured DNA in the absence of any stabilizing cation. The kinetics of the structural changes induced by these compounds could be followed by recording the changes in the CD signal as a function of time. The implications of the findings mentioned above are discussed in this paper.

Telomeric DNA consists of repetitive guanine-rich sequence which forms secondary structures based on reverse Hoogsteen-type base pairing involving four guanines in a planar arrangement termed a G-tetrad (*1*, *2*). The topology of these G-quadruplex structures depends on the DNA sequence, the number of telomeric repeats, the oligonucleotide concentration, and the stabilizing cation (*3*). The G-quadruplex forms of DNA do not serve as substrates for telomerase (*4*). Rather, telomerases are upregulated in 85−90% of cancer cells (*5*, *6*). In humans, the telomerase complex is composed of two essential components: telomerase reverse transcriptase (hTERT)[1] and an RNA component (hTR). In vitro experiments have shown that if the telomeric DNA is folded into a quadruplex, it becomes insensitive to the elongation by telomerase (*6*). In this context, G-quadruplex structures have been the focus of much medicinal chemistry research as attractive targets for the design of anticancer drugs (*7*, *8*).

G-Quadruplex DNA interactive compounds inhibit telomerase in vitro by stabilizing single-stranded 3′-telomere ends as a G-quadruplex (*5*, *6*). A strategy is being pursued to develop G-quadruplex promoter ligands, since the promoter ligands of certain genes also have quadruplex-forming sequence. The best example is a ligand called quarfloxacin (formerly CX-3543) that is now in phase II clinical trial as an anticancer agent. Most of the G-quadruplex DNA interacting compounds reported in literature have a central planar pharmacophore that is capable of stacking on the guanine tetrads via $\pi-\pi$ interactions and also have side chains, directed toward the quadruplex loops (*8*, *9*). Certain bis-triazole (*10*), bis-quinolinium (*11*), bis-urea (*12*), bis-indole (*13*), and bis-benzimidazole (*14*) compounds having selectivity toward quadruplex DNA were synthesized. Though a large number of G-quadruplex-stabilizing compounds have been reported, none of the above is known to induce the folding of the single-stranded guanine repeats into quadruplex DNA in the absence of any added cation and alter the topology or conformation of the quadruplex DNA. Recently, two anthracene-based molecules have been shown to induce the folding of human telomeric DNA sequence (*15*). G-Quadruplex structures can be intermolecular and intramolecular; the intramolecular quadruplexes are biologically more important since their structure may be altered upon interaction with appropriate ligands and proteins.

Previously, we have reported the DNA cleaving, duplex DNA binding, and topoisomerase inhibition properties by synthetic organic small molecules, including those based on benzimidazoles (*16*−*23*). Herein, we report the design and synthesis of four newly synthesized bis-benzimidazole-based ligands (**EtBzMe**, **EtBzEt**, **HyBzMe**, and **HyBzEt**) (Figure 1) and present experimental evidence of quadruplex formation, stabilization, and structural alteration using an oligonucleotide sequence of

†This work was supported by J. C. Bose Fellowship grant (S.B.) of the Department of Science and Technology (DST), New Delhi, India. A.K.J. is thankful to Department of Biotechnology (DBT), New Delhi, India for a Postdoctoral Fellowship.

*To whom correspondence should be addressed. E-mail: sb@orgchem.iisc.ernet.in. Phone: (91)-80-22932664. Fax: (91)-80-22930529.

[1]Abbreviations: hTERT, telomerase reverse transcriptase; NMR, nuclear magnetic resonance (spectroscopy); DMSO-d_6, dimethyl sulfoxide (deuterated); IR, infrared (spectroscopy); HRMS, high-resolution mass spectrometry; CD, circular dichroism spectropolarimetry; PAGE, polyacrylamide gel electrophoresis; T_{20}, 5′-TTT TTT TTT TTT TTT TTT TT-3′.

Published on Web 09/04/2009

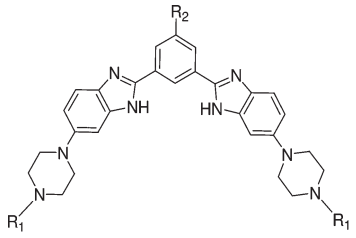

EtBzMe $R_1 = CH_3, R_2 = OCH_2CH_3$

EtBzEt $R_1 = CH_2CH_2OH, R_2 = OCH_2CH_3$

HyBzMe $R_1 = CH_3, R_2 = OH$

HyBzEt $R_1 = CH_2CH_2OH, R_2 = OH$

FIGURE 1: Molecular structures of the ligands used in this study.

Tetrahymena thermophilia by the above ligands even in the absence of any added salt.

EXPERIMENTAL PROCEDURES

Materials. All the starting materials were purchased from either Sigma-Aldrich or E-Merck. All solvents were from Merck, and they were distilled and/or dried prior to use whenever necessary.

General Spectrometric Characterization. NMR spectra were recorded on a Bruker AMX (300 or 400 MHz) spectrometer. IR spectra were recorded on FTIR Perkin-Elmer Spectrum GX spectrometer. Melting points were taken on a Buchi melting point B540 apparatus. Mass spectra were recorded on a Micromass Q-TOF Micro TM spectrometer.

Oligonucleotides. HPLC-purified oligodeoxyribonucleotides (ODN) of sequences $d(T_2G_4)_4$ and $d(T_{20})$ were purchased from Sigma, Genosys (Bangalore, India). Their purity was confirmed using a high-resolution sequencing gel. The molar concentration of each ODN was determined from absorbance measurements at 260 nm based on molar extinction coefficients (ε_{260}) of 229000 $M^{-1}\cdot cm^{-1}$ and 148400 $M^{-1}\cdot cm^{-1}$ for $d(T_2G_4)_4$ and $d(T_{20})$, respectively.

G-Quadruplex Formation. Single-stranded $d(T_2G_4)_4$ was dissolved in required buffer at the indicated concentration. The solution was first heated to 90 °C for 5 min and then cooled slowly to room temperature over a period of 24 h.

Chemistry. (*i*) *5-Hydroxyisophthalic Acid Dimethyl Ester* (***2***). 5-Hydroxyisophthalic acid (**1**, 9.1 g, 50 mmol) was refluxed for 4 h in dry methanol (20 mL) in the presence of a catalytic amount of concentrated H_2SO_4. Solvent was evaporated, and the residue was dissolved in water, neutralized with a saturated solution of sodium bicarbonate, and then extracted with ethyl acetate to yield 10.8 g of the desired compound as a white solid (96% yield): mp 154.2 °C; IR 3427.2, 2830, 2876, 1722.3, 1590, 1455, 1281 cm^{-1}; ^1H NMR ($CDCl_3$) δ 8.26 (s, 1H), 7.62 (s, 2H), 5.1 (s, 1H), 3.9 (s, 6H); Q-TOF HRMS found *m*/*z* 210.0612, calcd *m*/*z* 210.0528 ([M]).

(*ii*) *5-Ethoxyisophthalic Acid Dimethyl Ester* (***3***). Compound **2** (840 mg, 4 mmol) and ethyl bromide (654 mg, 6 mmol) were dissolved in dry acetonitrile (15 mL) in the presence of K_2CO_3 (600 mg) in a sealed tube and refluxed for 12 h. Solvent was evaporated, and the residue was dissolved in water, washed with a sodium bicarbonate solution, and then extracted with ethyl acetate to yield 932 mg of the desired compound as a white solid (98% yield): mp 102 °C; IR 2930, 2879, 1728.2 1594, 1456, 1281 cm^{-1}; ^1H NMR ($CDCl_3$) δ 8.24 (s, 1H), 7.72 (s, 2H), 4.1 (q, 2H, J = 6.6 Hz), 3.9 (s, 6H), 1.44 (t, 3H, J = 6.9 Hz); Q-TOF HRMS found *m*/*z* 262.0805, calcd *m*/*z* 262.0817 ($[M + Na]^+$).

(*iii*) *4-[4-(2-Hydroxyethyl)piperazin-1-yl]benzene-1,2-diamine* (***9***). (2-Hydroxyethyl)piperazine (520 mg, 4 mmol), 4-chloro-2-nitroaniline (690 mg, 4 mmol), and K_2CO_3 (610 mg) were taken in dry DMF (10 mL) and heated at 110 °C for 12 h. The reaction mixture was then cooled and poured on crushed ice (70 g) to yield a yellow precipitate, which was collected by filtration. The residue was crystallized in ethyl acetate to give 2-[4-(3-amino-4-nitrophenyl)piperazin-1-yl]ethanol (**7**, 767 mg, 72% yield): mp 175−176 °C; IR 3445, 3285, 3153, 1625, 1572 cm^{-1}; ^1H NMR (DMSO-d_6) δ 7.8 (s, 1H), 6.4 (s, 1H), 6.1 (s, 1H), 3.6 (b, merged with DMSO, 6H), 2.6 (b, 6H); Q-TOF HRMS found *m*/*z* 237.1461, calcd *m*/*z* 237.1457 ($[M + H]^+$).

The required quantity of **7** was dissolved in ethanol and hydrogenated over a catalytic amount of 10% Pd/C to yield **9**, and the resulting solution of **9** was used for further reaction as such each time.

(*iv*) [*3-Ethoxy-5-(hydroxymethyl)phenyl*]*methanol* (***10***). **3** (238 mg, 1 mmol) was dissolved in THF (6 mL), and lithium aluminum hydride (57 mg, 1.5 mmol) was added under ice-cold conditions. The reaction mixture was allowed to come to room temperature and stirred for 12 h. A dilute HCl solution was added to break the complex and decompose the unreacted excess of LAH and stirred for 0.5 h, and then the resulting solution was extracted with ethyl acetate to give 137 mg of **10** as a white solid (75% yield): mp 124−125 °C; IR 3347.9, 2930.5, 2878, 1598.3, 1455.2 cm^{-1}; ^1H NMR ($CDCl_3$) δ 6.91 (s, 1H), 6.82 (s, 2H), 4.65 (s, 4H), 4.04 (q, 2H, J = 6.5 Hz), 1.39 (t, 3H, J = 6.8 Hz); Q-TOF HRMS found *m*/*z* 206.0810, calcd *m*/*z* 206.0908 ($[M + Na]^+$).

(*v*) *3,5-Bis(hydroxymethyl)phenol* (***11***). **2** (210 mg, 1 mmol) was dissolved in THF (6 mL), and lithium aluminum hydride (57 mg, 1.5 mmol) was added under ice-cold conditions. The reaction mixture was allowed to come to room temperature and stirred for 12 h. A dilute HCl solution was added to break the complex and decompose the unreacted excess of LAH and stirred for 0.5 h, and then resulting solution was extracted with ethyl acetate to give 119 mg of **11** as an off-white solid (77% yield): mp 175−176 °C; IR 3349, 2930, 2879, 1599, 1455 cm^{-1}; ^1H NMR ($CDCl_3$) δ 7.43 (s, 1H), 6.77 (s, 2H), 4.55 (s, 4H); Q-TOF HRMS found *m*/*z* 177.0529, calcd *m*/*z* 177.0530 ($[M + Na]^+$).

(*vi*) *5-Ethoxybenzene 1,3-Dicarbaldehyde* (***12***). Compound **10** (91 mg, 0.5 mmol) was dissolved in a mixture of DCM and THF (6:4, 10 mL); 3 equiv of pyridinium chlorochromate (PCC) was added to this solution, and some silica was also added. The solution was stirred at room temperature for 1 h and then directly loaded on a silica gel column, and the required product (71 mg, 80% yield) was eluted with DCM as an off-white solid: mp 208−209 °C; IR 2932, 2875, 1676, 1599, 1442 cm^{-1}; ^1H NMR ($CDCl_3$) δ 9.92 (s, 2H), 8.9 (s, 1H), 7.5 (s, 2H), 3.98 (q, 2H, J = 6.4 Hz), 1.4 (t, 3H, J = 6.8 Hz); Q-TOF HRMS found *m*/*z* 201.0528, calcd *m*/*z* 201.0530 ($[M + Na]^+$).

(*vii*) *5-Hydroxybenzene 1,3-Dicarbaldehyde* (***13***). Compound **11** (72 mg, 0.5 mmol) was dissolved in a 3:2 mixture of DCM and THF (10 mL); 3 equiv of pyridinium chlorochromate (PCC) was added to this solution, and some silica was also added. The solution was stirred at room temperature for 1 h and then directly loaded on a silica gel column, and the required product (62 mg, 81% yield) was eluted with DCM as an off-white gum: IR 3446, 2931.5, 2875.6, 1678, 1596, 1439 cm^{-1}; ^1H NMR ($CDCl_3$) δ 9.9 (s, 2H), 8.0 (s, 1H), 7.6 (s, 2H), 5.1 (s, 1H); Q-TOF HRMS found *m*/*z* 173.0220, calcd *m*/*z* 173.0217 ($[M + Na]^+$).

(*vii*) *General Method for the Synthesis of 1,3-Phenylene-Bis(piperazinyl benzimidazole) Derivatives* (***EtBzMe***, ***EtBzEt***, ***HyBzMe***, *and* ***HyBzEt***). To a freshly prepared solution of either 4-(4-methylpiperazin-1-yl)benzene-1,2-diamine **8** (synthesized as described in ref *24*) or **9** was added 0.5 equiv of the dialdehyde (**12** or **13**), and to this solution was added sodium metabisulfite ($Na_2S_2O_5$, 1 equiv) dissolved in a minimum quantity of water. The reaction mixture was refluxed for 7−8 h with stirring, then cooled to room temperature, and filtered through Celite. Ethanol was then removed under reduced pressure to yield the required crude product. This crude product was then purified by column chromatography (EtOAc/MeOH) on silica gel (70−220 mesh size) to yield the required product, each of which was found to be hygroscopic in nature.

(*ix*) *2,2′-(5-Ethoxy-1,3-phenylene)bis{5-[4-(2-methyl)-1-piperazinyl]-1H-benzimidazole}* (***EtBzMe***). Freshly prepared 4-(4-methylpiperazin-1-yl)benzene-1,2-diamine (**8**, 103 mg, 0.5 mmol) and **12** (44 mg, 0.25 mmol) and $Na_2S_2O_5$ (47 mg) were reacted as per the general protocol (171 mg yield, 62%): mp 286 °C; IR 3401, 3062, 2927, 1625, 1497, 1443 cm^{-1}; ^1H NMR (DMSO-d_6) δ 12.90 (b, 2H), 8.57 (s, 2H), 7.78 (s, 2H), 7.55 (d, 1H, J = 6 Hz), 7.2 (s, 1H), 6.89 (m, 3H), 4.25 (q, 2H, J = 5 Hz), 3.4 (bs, 8H), 2.8 (bs, 8H), 1.4 (t, 3H, J = 5.8 Hz); ^{13}C NMR (DMSO-d_6) δ 159.23, 150.41, 149.96, 147.24, 138.1, 132.19, 119.02, 116.64, 114.60, 112.76, 97.63, 63.19, 53.64, 48.55, 43.95, 14.63; Q-TOF HRMS found m/z 551.3245, calcd m/z 551.3247 ($[M + H]^+$). Anal. Calcd for $C_{32}H_{38}N_8O \cdot 0.5H_2O$: C, 68.67; H, 7.02; N, 20.02. Found: C, 68.70; H, 6.69; N, 19.92.

(*x*) *2,2′-(5-Ethoxy-1,3-phenylene)bi{5-[4-(2-hydroxyethyl)-1-piperazinyl]-1H-benzimidazole}* (***EtBzEt***). Freshly prepared 4-[4-(2-hydroxyethyl)-piperazin-1-yl]benzene-1,2-diamine (**9**, 118 mg, 0.5 mmol) and **12** (44 mg, 0.25 mmol) and $Na_2S_2O_5$ (47 mg) were reacted as per the general protocol (186 mg yield, 61%): mp > 290 °C; IR 3480, 3400, 3059, 2920, 1619, 1496, 1442 cm^{-1}; ^1H NMR (DMSO-d_6) δ 12.50 (b, 2H), 8.57 (s, 2H), 7.8 (s, 2H), 7.6 (d, 1H, J = 6 Hz), 7.2 (s, 1H), 6.85 (m, 3H), 4.26 (q, 2H, J = 5.3 Hz), 3.6 (bs, 12H), 3.15 (bs, 8H), 2.65 (bs, 4H), 1.4 (t, 3H, J = 5.9 Hz); ^{13}C NMR (DMSO-d_6) δ 159.24, 149.53, 148.06, 137.92, 132.25, 118.94, 116.52, 113.63, 112.61, 97.19, 79.2, 63.63, 53.14, 48.53, 40.14, 14.67; Q-TOF HRMS found m/z 611.3477, calcd m/z 611.3458 ($[M + H]^+$). Anal. Calcd for $C_{34}H_{42}N_8O_3 \cdot H_2O$: C, 64.95; H, 7.05; N, 17.82. Found: C, 65.0; H, 7.10; N, 17.78.

(*xi*) *2,2′-(5-Hydroxy-1,3-phenylene)bis{5-[4-(2-methyl)-1-piperazinyl]-1H-benzimidazole}* (***HyBzMe***). Freshly prepared 4-(4-methylpiperazin-1-yl)benzene-1,2-diamine (**8**, 103 mg, 0.5 mmol) and **13** (38 mg, 0.25 mmol) and $Na_2S_2O_5$ (47 mg) were reacted as per the general protocol: (157 mg yield, 60%): mp > 290 °C; IR 3631, 3400, 2834, 2731, 1598, 1456, 1241 cm^{-1}; ^1H NMR (DMSO-d_6) δ 10.5 (b, 2H), 8.50 (s, 2H), 7.7 (s, 2H), 7.5 (d, 1H, J = 6 Hz), 7.03 (s, 1H), 6.90 (m, 3H), 3.62 (bs, 8H), 3.15 (bs, 8H), 2.65 (bs, 6H); ^{13}C NMR (DMSO-d_6) δ 158.17, 150.53, 146.39, 136.20, 132.02, 119.01, 115.48, 114.13, 97.20, 79.24, 61.23, 52.41, 47.25, 42.07; Q-TOF HRMS found m/z 523.2933, calcd m/z 523.2934 ($[M + H]^+$). Anal. Calcd for $C_{30}H_{34}N_8O \cdot H_2O$: C, 66.64; H, 6.71; N, 20.73. Found: C, 66.70; H, 6.78; N, 20.80.

(*xii*) *2,2′-(5-Hydroxy-1,3-phenylene)bis{5-[4-(2-hydroxyethyl)-1-piperazinyl]-1H-benzimidazole}* (***HyBzEt***). Freshly prepared 4-[4-(2-hydroxyethyl)piperazin-1-yl]benzene-1,2-diamine (**9**, 118 mg, 0.5 mmol) and **12** (38 mg, 0.25 mmol) and $Na_2S_2O_5$ (47 mg) were reacted as per the general protocol (180 mg yield, 62%): mp > 290 °C; IR 3460, 3400, 3959, 2836, 1633, 1455, 1239 cm^{-1}; ^1H NMR (DMSO-d_6) δ 13.0 (b, 2H), 8.5 (s, 2H), 7.8 (s, 2H), 7.6 (d, 1H, J = 6 Hz), 7.2 (s, 1H), 6.9 (m, 3H), 5.4 (s, 1H), 3.8 (bs, 12H), 3.3 (bs, 8H), 2.55 (bs, 4H); ^{13}C NMR (DMSO-d_6) δ 158.24, 150.53, 146.46, 137.82, 131.98, 119.04, 115.52, 115.32, 114.11, 96.19, 57.83, 55.32, 51.48, 47.07; Q-TOF HRMS found m/z 583.3144, calcd m/z 583.3145 ($[M + H]^+$). Anal. Calcd for $C_{32}H_{38}N_8O_3 \cdot 1.5H_2O$: C, 63.04; H, 6.78; N, 18.38. Found: C, 63.00; H, 6.80; N, 18.41.

Computational Details. All four molecules were computed for their energy-minimized structures in the aqueous phase using the B3LYP/6-31G* level of theory in Gaussian 03 (*25*). Aqueous-phase calculation was performed using the Onsager model taking the dielectric constant of the medium to be 78.4.

Circular Dichroism Spectroscopy. CD experiments were performed on a Jasco J-815 CD spectropolarimeter in a 10 mm path length quartz cell at 20 °C. The quadruplex (4 μM) solution in 10 mM sodium cacodylate with 100 mM LiCl (pH 7.3) or 10 mM Tris-HCl containing 100 mM NaCl or 100 mM KCl (pH 7.3) was taken in the cell and prior to experiments, and then the drug was added to DNA structures and incubated for 30 min to achieve maximum binding for the drug−DNA complexes. The stock solutions of new ligands were in DMSO and diluted in the required buffer prior to use. Spectra were recorded from 220 to 450 nm, with a scan speed of 50 nm/min, and an average of three scans was recorded.

T_m *Studies*. T_m measurements were performed on a Jasco J-810 CD spectropolarimeter in a quartz cell with a path length of 10 mm equipped with a thermo programmer. CD change was monitored at 295 and 260 nm (for the quadruplex without drugs) and at 266 nm for the drug−DNA complex, while the temperature was increased from 20 or 25 to 75 °C at a rate of 1.0 °C/min with a stability of 0.2 °C. The buffer consisted of 10 mM sodium cacodylate containing 100 mM LiCl (pH 7.3). The transition melting temperature (T_m) was determined by the first-derivative curve of the CD versus temperature plot. An average of three melting curves was recorded, and it was within the experimental error of 1.0 °C. The stock solutions of each new ligand were prepared in DMSO and diluted in the required buffer prior to use. The drug:DNA ratio was 3 and 5, and the ODN strand concentration was 2 μM.

Fluorescence Spectroscopy. Fluorescence spectra were recorded on a Hitachi F-4500 spectrophotometer using quartz cells with a path length of 1 cm. One milliliter of the respective 4 μM drug solution in 10 mM sodium cacodylate with 100 mM LiCl (pH 7.3) was taken in the cell, and quadruplex was added successively from a 10 μM stock solution in the same buffer (4 μL each time). Titrations were stopped when there was no change in fluorescence intensity after three successive additions. A 20 min incubation time was given after each addition. All spectra were recorded at 25 °C.

Absorption Titration Experiments. Binding assays were performed with preformed $d(T_2G_4)_4$ quadruplex in 10 mM Tris-HCl, with 100 mM KCl and 0.1 mM EDTA buffer, and with [(5′-$CGT_{13}GC$-3′)/(5′-$GCA_{13}CG$-3′)] duplex in 10 mM Tris-HCl, with 100 mM NaCl and 0.1 mM EDTA buffer (pH 7.3). The ligand solution (50 μM, 500 μL) was titrated by stepwise addition of aliquots of the DNA solution (4 μM). After each addition, the mixture was incubated at 25 °C for 15 min before measurement. The fractional decrease in absorbance at 325 nm for each [DNA]/[ligand] ratio was normalized using

$$\Delta A = (A_{free} - A)/(A_{free} - A_{sat})$$

where A_{free} and A_{sat} are the absorbance for the free and fully bound ligands, respectively. The fraction of bound drug α (on a

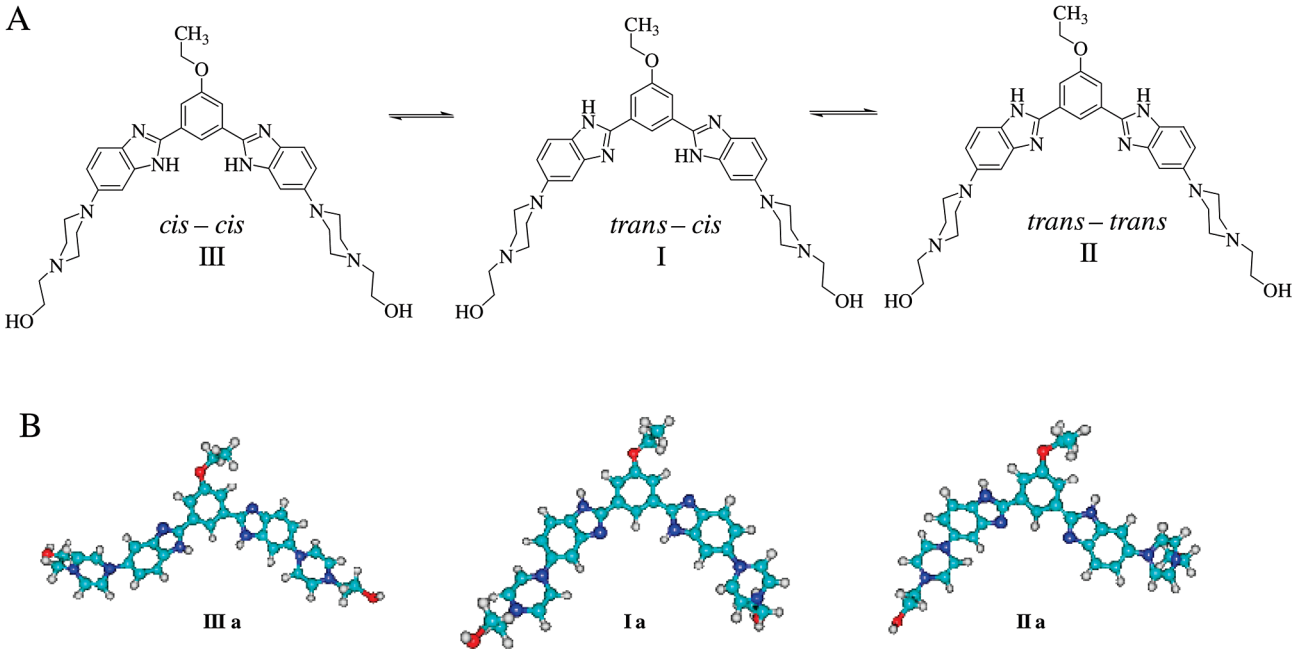

FIGURE 2: (A) Three possible conformers of **EtBzEt**. (B) B3LYP/6-31G* minimized structures in aqueous solution.

0−1 scale) at each intermediate titration position is given directly by the relative ΔA hypochromicity term (*26*). The concentration of free ligand is calculated using

$$C_f = (1-\alpha)C$$

where C is the total ligand concentration (fixed at 50 μM) and can be used to determine the binding ratio r, defined as $(C - C_f)$/[DNA]. Titration data were cast into the form of Scatchard plots of r/C_f versus r for analysis, where K_a is the intrinsic equilibrium binding constant and n is an exclusion parameter that defines the number of ligand molecules bound per DNA quadruplex. Data were also fitted using the simpler, linear Scatchard equation (eq 1)

$$r/C_f = K_a(n-r) \quad (1)$$

Polyacrylamide Gel Electrophoresis. The single-stranded $d(T_2G_4)_4$ and T_{20} marker (10 pmol/μL each) were 5′-^{32}P labeled with [γ-^{32}P]ATP (Amersham) and purified by chromatography on Sephadex G-50. For G-quadruplex DNA, labeled DNA (10000 cpm tracer) was mixed with unlabeled single-stranded DNA to a concentration of 5 μM in buffer containing 100 mM LiCl, NaCl, or KCl, Tris, and 1 mM EDTA (pH 7.3), and the reaction volume was 20 μL. Reaction mixtures were heated individually at 90 °C for 10 min, cooled slowly to 24 °C, and incubated for 24 h in the presence of different ligands at various concentrations. The ligand incubation with DNA was terminated by the addition of 5 μL of gel loading buffer (30% glycerol, 0.1% bromophenol blue, and 0.1% xylene cyanol). Ten microliters of the subsequent ligand−quadruplex complexes was analyzed on a 12% native PAGE gel (the gel was prerun for 30 min). Electrophoresis was conducted for 3 h at 4 °C at 80 V in 0.5× TBE buffer (pH 7.3) containing 20 mM NaCl or KCl. Gels were dried and visualized using a phosphorimager.

RESULTS

Bisbenzimidazole compounds are known to have cell and nuclear membrane permeability along with other important biological properties. Currently, these are used in cytometry and in staining of vertebrate chromosomes (*27*−*32*). Herein, we decided to prepare a novel class of molecules based on conformationally flexible benzimidazoles, based on the 1,3-substituted system, which possess an extended delocalized π-electron system, and tertiary amines that are protonated at physiological pH. These molecules also contain functions that are able to form hydrogen bonds with the phosphate backbone and bases of the loops, properties that are required for the stabilization of G-tetrads (*33*, *34*).

The compounds used in this study have a symmetrical, V-shaped central core, which has been shown to be important for quadruplex stabilization (*10*−*14*). In this case, each of the ligands can adopt three conformations because of geometric freedom (Figure 2). Therefore, for the computation (B3LYP/6-31G*) of the energy-minimized structures in aqueous solution, three relevant conformations were considered: (i) one in which one of the benzimidazole NH groups is located on the inner (concave) edge and the other one on the outer (convex) edge (*cis*−*trans*) (I), (ii) one in which both the benzimidazole NH groups are at the outer (convex) edge (*trans*−*trans*) (II), and (iii) one in which both the benzimidazole NH groups are located on the inner concave edge (*cis*−*cis*) (III) (Figure 2 and Supporting Information). Conformation I was found to be most stable among the three conformers in the solution phase for all the compounds. Importantly, these compounds exhibit a nearly planar central core [based on the dihedral angles (Supporting Information)], and their molecular sizes were comparable to that of the G-quartet (Supporting Information) of the crystal structure obtained from a human telomeric quadruplex DNA sequence (*35*).

For the syntheses of these compounds, commercially available 5-hydroxyisophthalic acid (**1**) and 5-chloro-2-nitroaniline were employed as the key starting materials. Compound **1** was first converted into dimethyl ester **2**, which was then ethoxylated at the phenolic end to afford **3**. Compounds **2** and **3** were separately then reduced to furnish corresponding alcohols **10** and **11**, respectively. **10** and **11** were then oxidized to yield key dialdehydes **12** and **13**, respectively. For the synthesis of the other fragment for coupling

Scheme 1: Synthesis of Compounds Used in This Study[a]

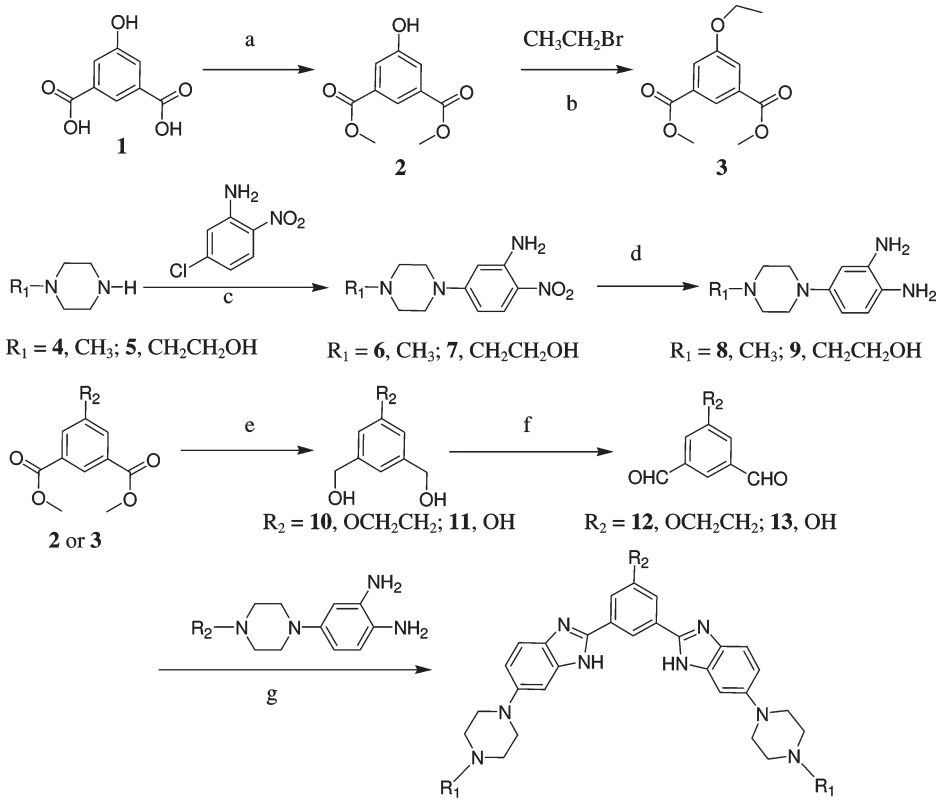

[a](a) Methanol, H_2SO_4, reflux; (b) K_2CO_3, CH_3CN, reflux (sealed tube); (c) K_2CO_3, DMF, 110 °C; (d) H_2, Pd/C (10%); (e) LAH, THF, room temperature; (f) PCC, DCM, or DCM/THF, room temperature; (g) $Na_2S_2O_5$, EtOH, reflux.

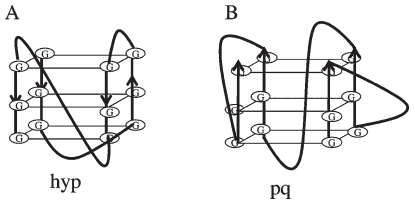

FIGURE 3: Schematic models of G-quadruplex structures formed under different ionic conditions. Hybrid intramolecular quadruplex "hyq" formed in Na^+ solution (A) and proposed parallel intramolecular quadruplex "pq" (B).

with the dialdehydes, 5-chloro-2-nitroaniline was reacted with either 1-methylpiperazine or 1-(2-hydroxyethyl)piperazine to produce compounds **6** and **7** which were hydrogenated over 10% Pd/C to afford diamines **8** and **9**, respectively. Subsequent oxidative condensation of diamines **8** and **9** with dialdehydes **12** and **13** yielded the desired compounds **EtBzMe**, **EtBzEt**, HyBzMe, and **HyBzEt**, respectively (Scheme 1). All the new and final compounds were fully characterized using IR, ^{1}H NMR, ^{13}C NMR, and HRMS, and the resulting structural data were consistent with their given structures.

Telomeric repeats of *T. thermophila* are known to form various types of G-quadruplex structures. We selected the single-stranded $d[T_2G_4]_4$ of *Tetrahymena* as a model for this investigation since this sequence has been shown to exhibit an interesting and wide range of structural polymorphism depending upon whether the quadruplex formation occurs in the presence of Na^+ or K^+ (*36*−*38*). Because of this structural polymorphism, the *Tetrahymena* quadruplex has been used as a model system to study quadruplex-stabilizing ligands in other reports also (*39*, *40*). The predominant species formed in buffer containing Na^+ was a fold-over intramolecular structure (Na^+-quad) with three stacked G-quartets linked by two lateral loops and a propeller loop, giving rise to a structure with three parallel strands and one antiparallel strand (*37*, *41*) (Figure 3A). Such a mixed type of hybrid quadruplex DNA displays a circular dichroism (CD) profile in maxima at 295 nm (antiparallel characteristics) and 260 nm (parallel characteristics) and a minimum around 242 nm of approximately equal intensity (*37*, *41*). In contrast, formation of quadruplex DNA in the presence of K^+ (K^+-quad) gave rise to a mixture of both multistrand intermolecular and unimolecular (intramolecular) quadruplex structure (Figure 3). This was marked by the formation of an intense positive band at 265 nm, a shoulder at 295 nm, and a minimum at 242 nm (*41*, *42*).

The monovalent Na^+ and K^+ ions are known to induce and stabilize the G-quadruplex DNA structure. Li^+ ions induce G-quadruplex formation, but they have very little effect on quadruplex stability (*43*). To explore the effect of our compounds on the stability and structural change, if any, of G-quadruplex DNA, we have chosen buffer solutions having mainly LiCl [10 mM sodium cacodylate having 100 mM LiCl and 0.1 mM EDTA (pH 7.3)]. For CD titrations, we have also used a NaCl or KCl [10 mM Tris containing 100 mM NaCl or 100 mM KCl and 0.1 mM EDTA (pH 7.3)] solution. CD spectra of the G-quadruplex formed with NaCl and KCl matched with that of the previous studies (*42*); in the CD spectra of the quadruplex formed with LiCl, the peak at 295 nm was less intense than the

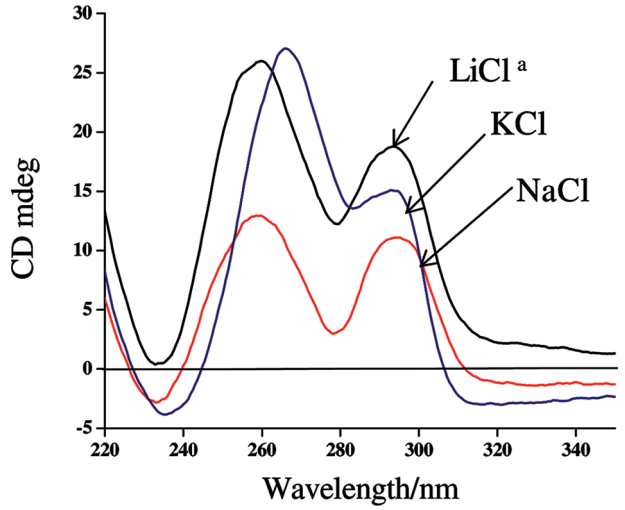

FIGURE 4: CD spectra of the quadruplex formed by *Tetrahymena* telomeric repeat $d(T_2G_4)_4$ (4 μM strand concentration) in the presence of indicated ions (100 mM). The mixture for the black trace included 10 mM Na^+ and 100 mM Li^+.

peak at 260 nm, but both were more intense than the peaks of NaCl-stabilized quadruplex DNA (Figure 4).

CD Titrations. We performed titrations of each compound with the preformed quadruplex DNA in buffer containing LiCl (10 mM Na^+ and 100 mM Li^+). Both spectral peaks (260 and 295 nm) started merging to generate a peak at 266 nm, beginning with the addition of the first aliquot of **EtBzMe** (Figure 5A). A shoulder (295 nm) that was formed at a drug:DNA ratio of 1 disappeared at a ratio of 2. A small negative peak also appeared near 242 nm. The intensity of the positive peak increased with subsequent addition of the compound, and it was nearly the same at ratios of 4, 5, and 6. Consequently, we decided to employ higher drug:DNA ratios. There was a dramatic spectral change at a ratio of 10. The intensity of the 266 nm peak started to decrease, and the intensity of the negative signal near 242 nm started to increase. An induced positive CD signal started to appear at 325 nm beyond a ratio of 12.5, the intensity of which increased on subsequent addition of the compound (Figure 5B). The titrations with **EtBzEt** also gave similar results (Figure 6), but it appeared as a completely merged peak following the addition of the first aliquot of **EtBzEt** only. There was no shoulder at 295 nm at a ratio of 1, and the peak at 266 nm was more intense after the addition of every aliquot. Compounds **HyBzMe** and **HyBzEt** showed similar results (Supporting Information).

To study the kinetics of structural conversion by **EtBzEt**, we monitored the buildup of the CD signal at 266 nm as a function of time. Since the CD profile of quadruplex DNA in the presence of LiCl shows complete structural conversion near a drug:DNA ratio of 10, we selected this ratio for the kinetic study. Under these conditions, the ellipticity at 266 nm increased steadily up to ~600 s, and then a plateau was reached in a monoexponential manner (Figure 7). A plot of $\log[(a_\infty - a_0)/(a_\infty - a_t)]$ versus time (t) afforded a straight line (correlation coefficient = 0.999) (Figure 7) indicating that the structural conversion of binding the quadruplex DNA by the ligand followed first-order kinetics. On the basis of this, a rate constant of 9.0×10^{-3} s^{-1} for this process was determined. Compound **HyBzEt** upon binding with $d(T_2G_4)_4$ also gave similar results (Supporting Information).

Next we performed the CD titrations using NaCl-stabilized quadruplex DNA. Upon addition of **EtBzEt**, there was a gradual red shift of the 260 nm peak and it stayed at 266 nm at a drug:DNA ratio of 4 (Figure 8A). There was a gradual decrease in the intensity of the 295 nm peak, and it remained as a shoulder up to a drug:DNA ratio of 5. A small negative peak also generated near 325 nm from a ratio of 3−5. The intensity of the 266 nm peak decreased dramatically beyond a ratio of 10 (Figure 8B). **EtBzMe** also gave similar results (Supporting Information).

We also performed CD titrations with KCl-stabilized quadruplex. At drug:DNA ratios of 5 and 10 in the presence of **EtBzMe** and **EtBzEt**, respectively, the intensity of the 266 nm peak decreased markedly as observed in the case of Li^+- and Na^+-stabilized quadruplex while the intensity of the 295 nm peak did

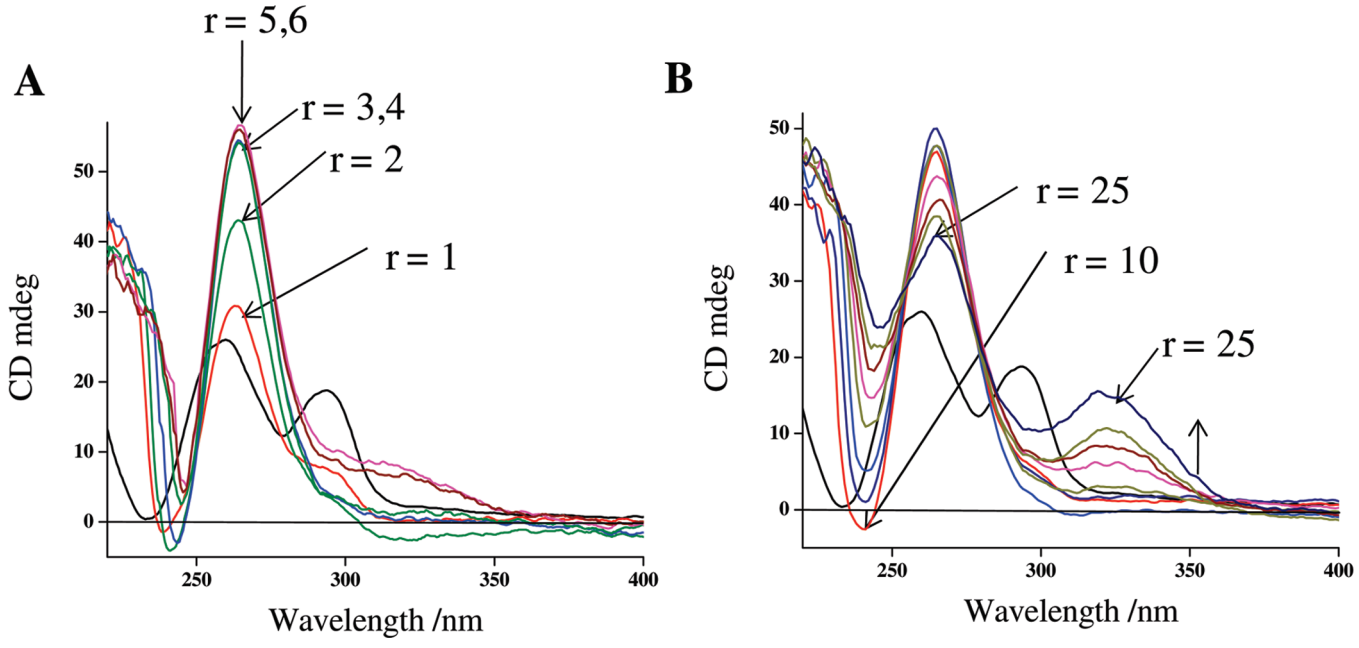

FIGURE 5: CD titrations of $d(T_2G_4)_4$ (strand concentration of 4 μM) in LiCl buffer [10 mM sodium cacodylate with 100 mM LiCl and 0.1 mM EDTA (pH 7.3)] with **EtBzMe** [from 4 to 24 μM **EtBzMe**, 4 μM addition each time (A), and from 40 to 100 μM **EtBzMe**, 10 μM addition each time (B)].

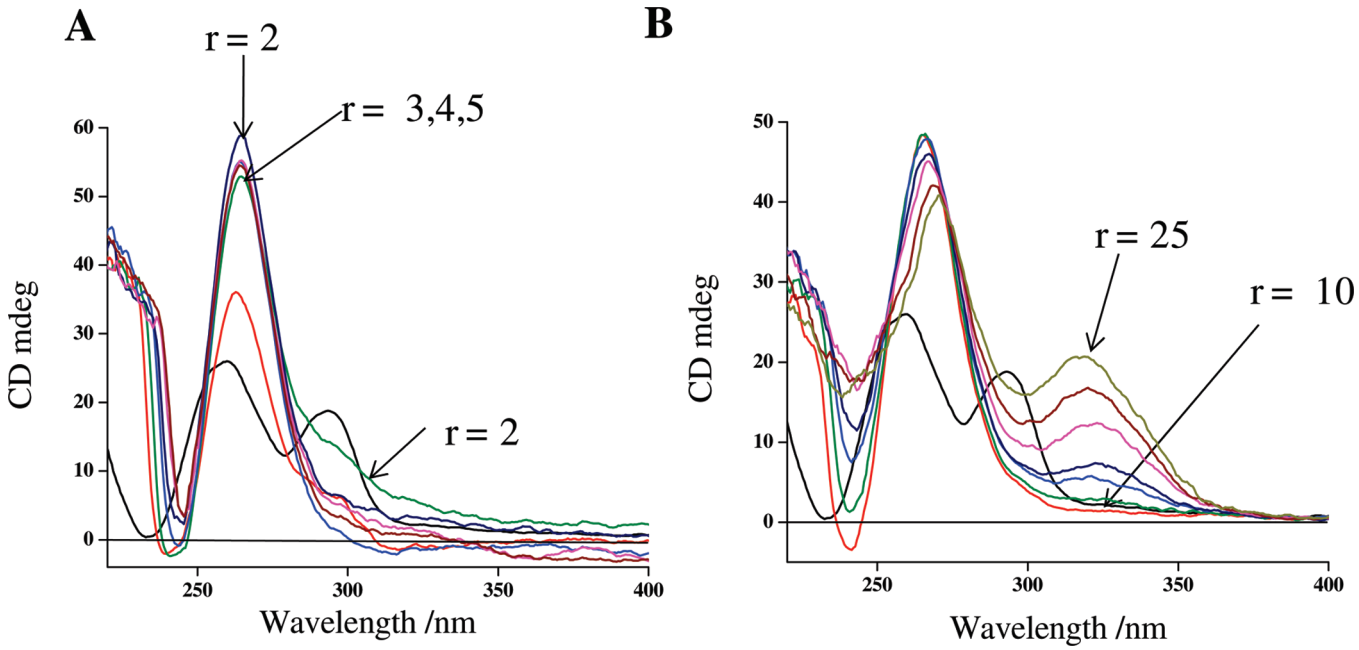

FIGURE 6: CD titrations of $d(T_2G_4)_4$ (strand concentration of 4 μM) in LiCl buffer [10 mM sodium cacodylate with 100 mM LiCl and 0.1 mM EDTA (pH 7.3)] with **EtBzEt** [from 4 to 24 μM **EtBzEt** (A) and from 40 to 100 μM **EtBzEt** (B)].

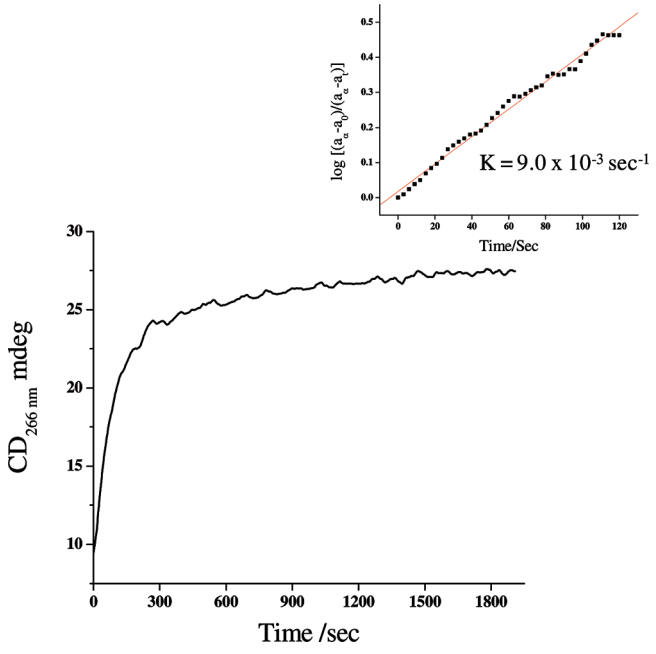

FIGURE 7: Time course study of $d(T_2G_4)_4$ (strand concentration of 4 μM) in LiCl buffer [10 mM sodium cacodylate with 100 mM LiCl and 0.1 mM EDTA (pH 7.3)] with 40 μM **EtBzEt** at 266 nm. The inset shows a plot of $\log[(a_\infty - a_0)/(a_\infty - a_t)]$ vs t (seconds) for the structural conversion of G-quadruplex DNA. Here, a_∞ is the ellipticity obtained after complete structural conversion, a_t the ellipticity obtained at time t, and a_0 the initial ellipticity observed at time zero.

not change significantly upon addition of the ligand (Supporting Information). The change was greater in the case of **EtBzEt**. The K^+-stabilized $d(T_2G_4)_4$ contains a mixture of intramolecular and intermolecular species (*36*, *38*, *41*), out of which the intermolecular quadruplex is highly stable. It appears that the addition of any of the compounds alters the ratio of these two species.

Next we wished to determine the nature of the DNA secondary structures that these drugs have induced in the absence of any added monovalent cations like Na^+, Li^+, or K^+. To single-stranded DNA, which contains no secondary structure (Figure 9A), was added **EtBzEt** at increasing concentrations. Addition of drug caused a pronounced red shift at 255−265 nm. An induced positive peak appeared near 325 nm at a drug:DNA ratio of 20. At higher ratios, the intensity of the 265 nm peak decreased and the induced CD signal became more prominent (Supporting Information). Time course experiments in the presence of **EtBzEt** and in the absence of stabilizing cations at a drug:DNA ratio of 10 also suggested the first-order type kinetics of such structural conversion (Figure 9B). On the basis of this, a rate constant of 7.43×10^{-3} s^{-1} was determined.

Fluorescence Titrations. Fluorescence titrations were conducted by adding a solution of each compound with the preformed quadruplex in LiCl buffer. The results obtained corroborate the evidence of binding of these compounds with the quadruplex DNA (Figure 10). Compound **EtBzEt** showed the highest relative increment, while **EtBzMe** and **HyBzEt** showed almost equal increments. The saturation point was near the DNA:drug ratio ($1/r$) of 0.13 or the drug:DNA ratio (r) of 7.7.

DNA Melting. Thermal denaturation studies again indicate the binding of the new compounds with the *Tetrahymena* $d(T_2G_4)_4$ quadruplex DNA. CD spectra of uncomplexed quadruplex had two positive peaks at 260 and 295 nm, respectively, in LiCl buffer (Figure 4). The CD melting curve at 295 nm was sigmoidal in nature, but at 260 nm, it was not sigmoidal (Figure 11A). Melting temperatures of the uncomplexed quadruplex at 295 and 260 nm were 36 and 39 °C, respectively (Table 1). Ligand-bound quadruplexes exhibited sigmoidal melting curves at 266 nm in all cases (Figure 11B).

Interestingly, the quadruplex of randomly structured $d(T_2G_4)_4$ in Tris buffer (without any stabilizing cation) in the presence of **EtBzEt** also exhibited a high melting temperature [45 °C (Table 1, entry 10)], which was even higher than that of the quadruplex formed in the presence of 100 mM LiCl.

Absorption Titration. The UV−vis titration spectra of all four compounds with the preformed G-quadruplex resulted in hypochromicity, which indicates a specific binding and strong stacking interaction with G-quadruplex DNA (*44*); on the other

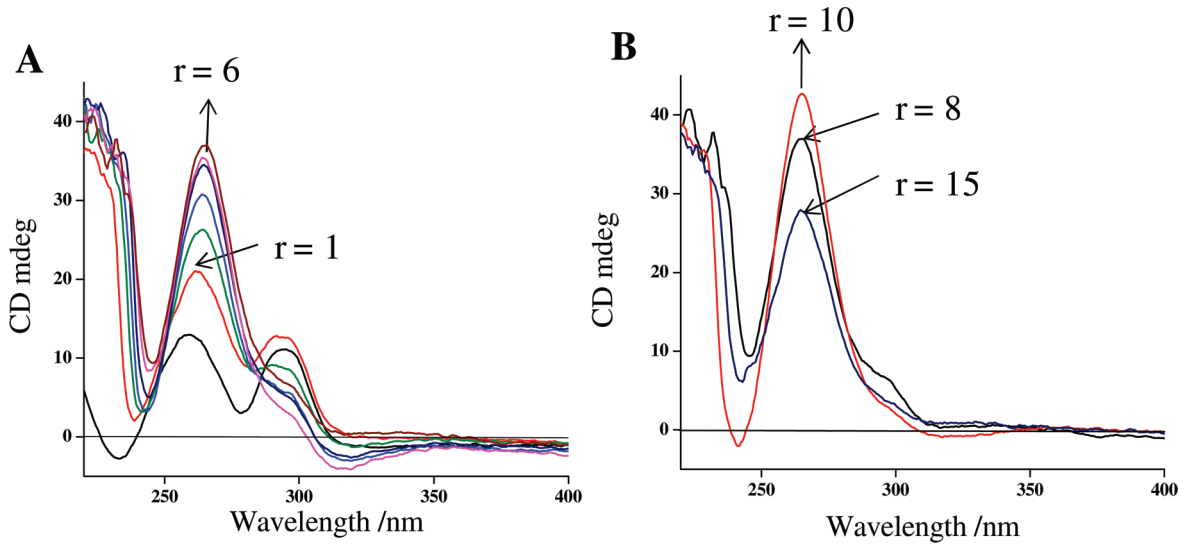

FIGURE 8: CD titrations of $d(T_2G_4)_4$ (strand concentration of 4 μM) in NaCl buffer [10 mM Tris-HCl (pH 7.3) with 100 mM NaCl and 0.1 mM EDTA] with **EtBzEt** (from 4 to 24 μM **EtBzEt** and then 40 and 60 μM **EtBzEt**).

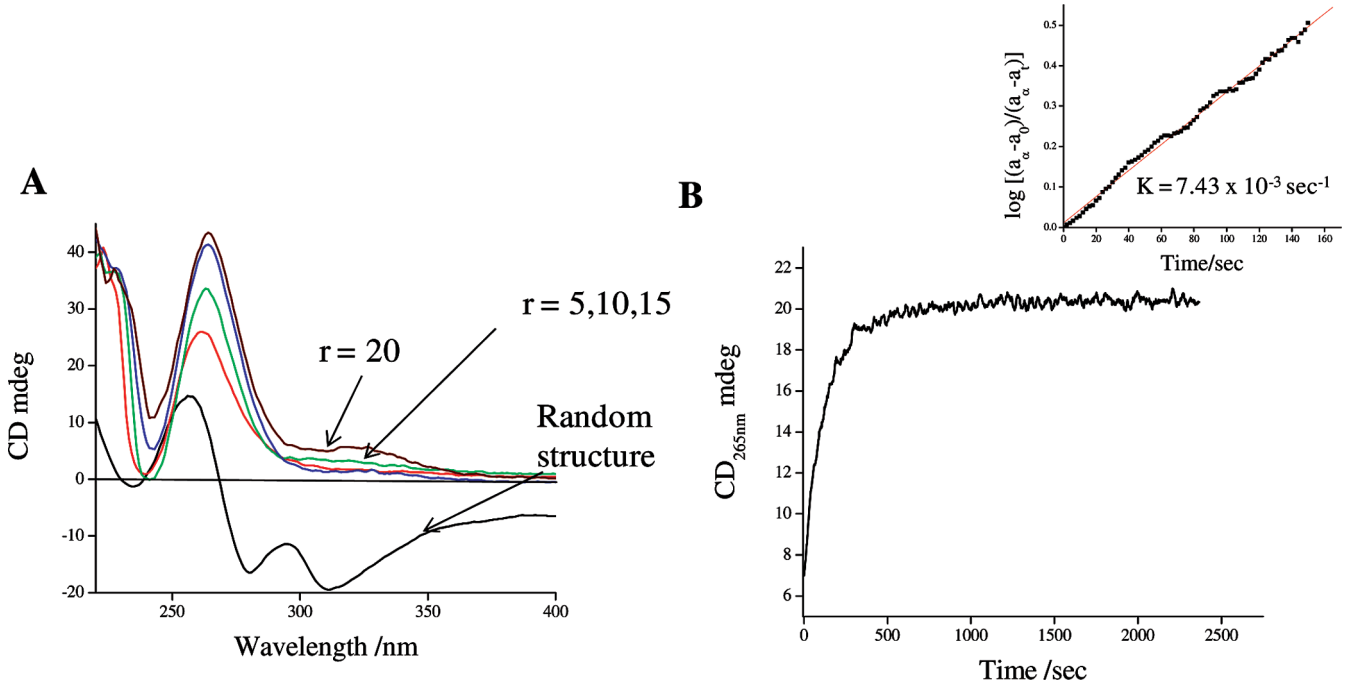

FIGURE 9: (A) CD titrations of $d(T_2G_4)_4$ (strand concentration of 4 μM) in Tris buffer [10 mM Tris and 0.1 mM EDTA (pH 7.3) without any added metal ion] with **EtBzEt** (from 20 to 80 μM **EtBzEt**). (B) Time course study of 4 μM strand with 40 μM **EtBzEt** at 265 nm. The inset shows a plot of $\log[(a_\infty - a_0)/(a_\infty - a_t)]$ vs t (seconds) for the structural conversion of G-quadruplex DNA. See Figure 7 for the definition of notations.

hand, we observed significantly less hypochromicity with duplex DNA.

The UV−vis titration results were converted into Scatchard plots (Supporting Information), and dissociation constants were determined by linear fitting. **EtBzEt** binds strongly to the G-quadruplex DNA showing a dissociation constant (K_D) of 5.32×10^5 M^{-1}, while for duplex DNA, the K_D was only 6.0×10^3 M^{-1}, indicating the weaker binding of the ligand with the duplex DNA (Table 2). Interestingly, we did not detect any significant binding with CT-DNA (data not shown) in absorption titrations.

Polyacrylamide Gel Electrophoresis. Finally, we prepared the quadruplex using 5′-^{32}P-end-labeled $d(T_2G_4)_4$ in all three buffers and resolved it on a 12% native polyacrylamide gel. Quadruplex formed in the presence of LiCl or NaCl formed largely single bands (Supporting Information) since it forms a hybrid intramolecular quadruplex under these conditions. The product from KCl has some higher bands too. It was supposed to form a mixture of intramolecular and intermolecular quadruplexes (*38*, *41*), but the intermolecular product was at a very low concentration under the conditions used here (Supporting Information). We have isolated the DNA from the major bands in the respective buffer for further experiments, but after isolation, we found heterogeneity in the quadruplexes. It is possible that the intramolecular quadruplexes are less stable, and this is consistent with earlier reports on the $d(T_2G_4)_4$ quadruplex, where heterogeneity was also evidenced after gel elution (*38*).

Electrophoresis of quadruplex DNA eluted from the NaCl-stabilized quadruplex showed the emergence of a new band after interaction with **EtBzEt** (Figure 12). We also compared the

mobility of the quadruplex with that of the T_{20} marker (Figure 13). **EtBzEt** showed complete conversion at a drug:DNA ratio of 5 with quadruplex formed in buffer with LiCl, but in the NaCl-stabilized quadruplex, complete conversion took place beyond a ratio of 10 (Figure 13).

DISCUSSION

CD titration results in Li^+ buffer suggest the conversion of the intramolecular parallel−antiparallel hybrid quadruplex into a parallel structure upon interaction with **EtBzEt** and **EtBzMe** (Figures 5 and 6), like the K^+-stabilized *Tetrahymena* quadruplex (*41*, *42*). Besides the planar G-quartet, quadruplexes also have other sites available for the interaction with a guest molecule (*45*). After complete conversion at a ratio of ~10, an induced CD signal appeared, which could be due to the interaction of the added compound with the chiral grooves of the quadruplex DNA. The side chains of the quadruplex binding compounds also have their role in groove binding (*46*, *47*). Benzimidazoles are known to cause DNA aggregation and undergo self-aggregation (*31*, *48*, *49*). At higher drug:DNA ratios, the magnitude of the induced CD signal increased significantly (Supporting Information), and it appeared either due to the formation of a distorted structure or due to aggregation.

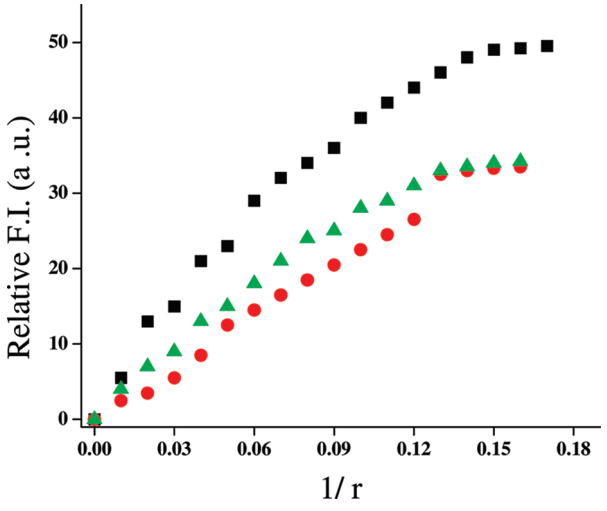

FIGURE 10: Relative increment in the fluorescence intensity of compounds (400 nM) in LiCl buffer [10 mM sodium cacodylate with 100 mM LiCl and 0.1 mM EDTA (pH 7.3)] with **EtBzMe** (red), **EtBzEt** (black), and **HyBzEt** (green). Quadruplex formed by $d(T_2G_4)_4$ was added from the stock with a strand concentration of 4 μM to the solution of the individual compound in the cuvette.

EtBzEt and **EtBzMe** also induced a conversion of the NaCl-stabilized intramolecular parallel−antiparallel hybrid quadruplex into a parallel structure (Figure 8), like the K^+-stabilized *Tetrahymena* quadruplex DNA (*38*), but since Na^+ stabilized the G-quadruplex, it prevented the change and structural conversion appeared above $r = 3$ only. Interestingly, **EtBzEt** induced the same secondary structure (parallel-stranded) in the absence of any stabilizing cation, as with the preformed quadruplex in the presence of Li^+ and Na^+ ions (Figure 9).

Incorporation of an electron-donating group on the phenyl ring enhanced the stability of the drug−DNA (duplex) complex (*31*). From the T_m data (Figure 11 and Table 1), it is clear that both the substitution at the central phenyl ring and the substitution at piperazinyl unit of symmetric bisbenzimidazoles have an important role in quadruplex stabilization. These compounds are also capable of inducing and stabilizing the parallel-stranded quadruplex with randomly structured $d(T_2G_4)_4$ without the help of any stabilizing cation (Figure 11A, green curve).

The strong stabilization properties of the compounds here could originate from their geometric complementarity with that of the G-quartet. The molecular size and geometry of these ligands may not be favorable for interaction with a base pair in duplex DNA, resulting in a strong preference for the quadruplex. Compounds would have positively charged amine groups under experimental conditions (pH 7.3). Recently, a crystal structure of BRACO-19 with the bimolecular human quadruplex has been reported showing the binding of the side chains of the compounds in the grooves of the quadruplex DNA (*46*). The substituted

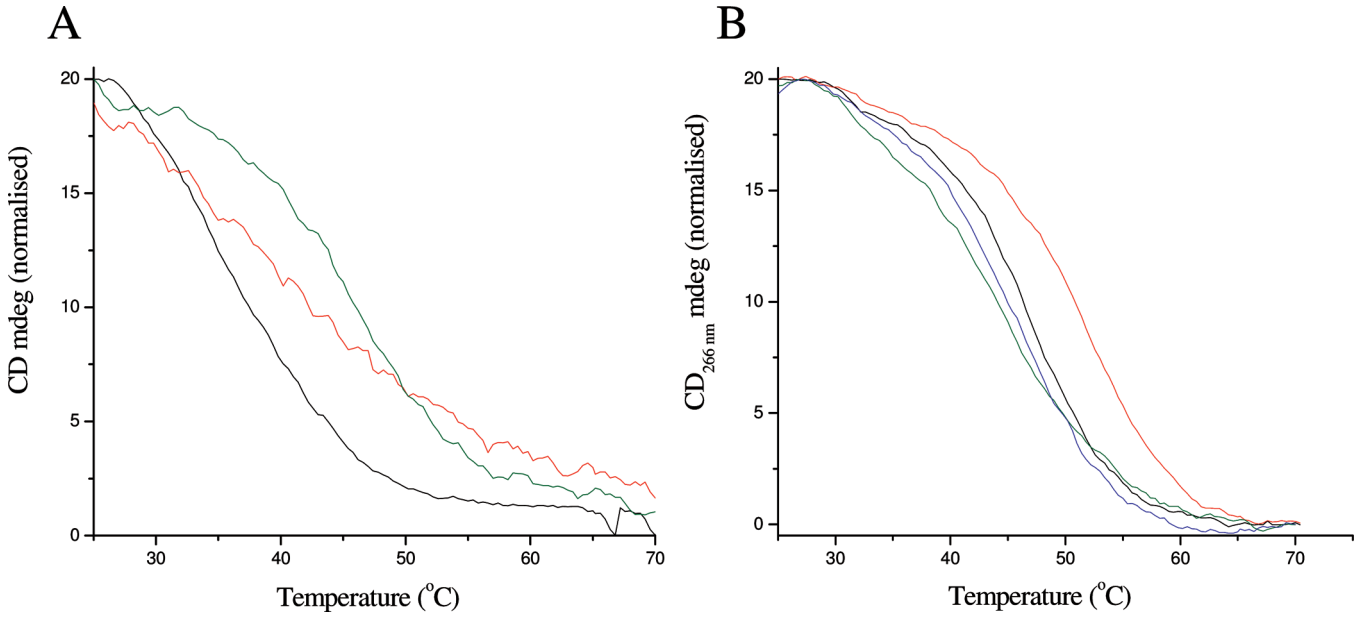

FIGURE 11: (A) Representative normalized CD melting profiles of *Tetrahymena* $d(T_2G_4)_4$ quadruplex (strand concentration of 2 μM) in LiCl buffer [10 mM sodium cacodylate with 100 mM LiCl (pH 7.3)] at 260 (red) and 295 nm (black) and with 10 μM **EtBzEt** in Tris buffer without any stabilizing ions (green). (B) Representative normalized CD melting profiles of the quadruplex (2 μM) with 10 μM compounds [**EtBzMe** (black), **EtBzEt** (red), **HyBzMe** (green), and **HyBzEt** (blue)] in the same buffer at 266 nm. Data have been normalized between 0 and 20 for clearance.

Table 1: Melting Temperatures (CD melting) of the *Tetrahymena* $d(T_2G_4)_4$ Quadruplex (strand concentration of 2 μM) Formed in LiCl Buffer [10 mM sodium cacodylate with 100 mM LiCl and 0.1 mM EDTA (pH 7.3)], except Entry 10, and the Quadruplex Complexed with 6 or 10 μM Compounds (**EtBzMe**, **EtBzEt**, **HyBzMe**, and **HyBzEt**) in the Same Buffer at 266 nm

			ΔT_m (°C) (at 266 nm)[b]	
	system	T_m (°C)[a]	260 nm	295 nm
1	2 μM $d(T_2G_4)_4$	36 at 295 nm (0.55) 39 at 260 nm (0.4)		
2	$d(T_2G_4)_4$ + **EtBzMe** (r^c = 3)	44.5 (0.45)	5.5	8.5
3	$d(T_2G_4)_4$ + **EtBzMe** (r = 5)	47 (0.6)	8	11
4	$d(T_2G_4)_4$ + **EtBzEt** (r = 3)	47 (0.3)	8	11
5	$d(T_2G_4)_4$ + **EtBzEt** (r = 5)	51.5 (0.5)	12.5	15.5
6	$d(T_2G_4)_4$ + **HyBzMe** (r = 3)	–	–	–
7	$d(T_2G_4)_4$ + **HyBzMe** (r = 5)	45 (0.35)	6	9
8	$d(T_2G_4)_4$ + **HyBzEt** (r = 3)	–	–	–
9	$d(T_2G_4)_4$ + **HyBzEt** (r = 5)	47 (0.4)	8	11
10	$d(T_2G_4)_4$-Tris + **EtBzEt** (r = 5)[d]	45 (0.45)		

[a]Melting temperatures were determined by first-derivative analysis. T_m values represent the average of three readings and were within the experimental error of ±1.0 °C. The numbers in parentheses are the estimated standard deviations. [b]ΔT_m values were obtained from the difference in melting temperatures of the ligand-bound and uncomplexed quadruplex DNA. [c]r is the drug:DNA concentration ratio. The DNA concentration was 2 μM in each case. [d]For entry 10, the quadruplex was formed in 10 mM Tris and 0.1 mM EDTA (pH 7.3) without any metal ion.

Table 2: Dissociation Constants (K_D) of All Four Compounds with the Preformed $d(T_2G_4)_4$ Quadruplex and [(5′-$CGT_{13}GC$-3′)/(5′-$GCA_{13}CG$-3′)] Duplex[a]

	K_D ($\times 10^5$ M^{-1})	
ligand	$d(T_2G_4)_4$	duplex
EtBzEt	5.32 ± 0.08	0.06 ± 0.02
EtBzMe	1.76 ± 0.6	0.045 ± 0.08
HyBzEt	0.89 ± 0.3	0.09 ± 0.05
HyBzMe	0.68 ± 0.12	0.058 ± 0.03

[a]Binding assays were performed with the preformed $d(T_2G_4)_4$ quadruplex in 10 mM Tris-HCl, with 100 mM KCl and 0.1 mM EDTA buffer, and with [(5′-$CGT_{13}GC$-3′)/(5′-$GCA_{13}CG$-3′)] duplex in 10 mM Tris-HCl, with 100 mM NaCl and 0.1 mM EDTA buffer (pH 7.3).

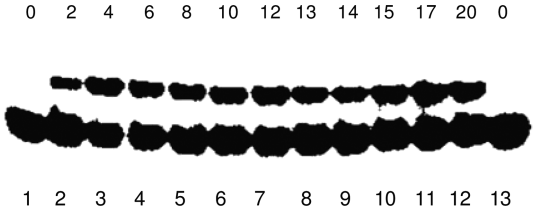

FIGURE 12: Emergence of a new band upon interaction of the indicated amount (over each lane) of **EtBzEt** (micromolar) with 5 μM $d(T_2G_4)_4$ quadruplex formed in 100 mM NaCl. Lanes 1 and 13 contained quadruplex alone.

piperazinyl side chains in this set of molecules may also interact with the quadruplex DNA grooves through hydrogen bonding. The stronger stabilization provided by **EtBzEt** could be due to the presence of an extra OH group at each end to form hydrogen bonds with the bases of G-quadruplex loops.

Compound **EtBzEt**, having an electron-donating ethoxy group at the phenyl ring and 2-hydroxyethyl group at the side chain piperazine units, provided the strongest stabilization in the series (Table 1), while **EtBzMe**, having an ethoxy group at the phenyl ring but a methyl group at the piperazinyl ring, provided less stabilization than **EtBzEt**. Similarly, **HybzEt**, having a 2-hydroxyethyl group at the piperazine unit, provided stronger stabilization of the quadruplex than **HyBzMe** having a methyl group at the piperazinyl side chain. The order of stabilization was as follows: **EtBzEt** > **EtBzMe** ≥ **HyBzEt** > **HyBzMe**.

The role of the electron-donating group in these compounds for quadruplex stabilization is a matter of interest. The compounds having electron-donating groups are often considered as good intercalators (*50*), since they have good $\pi-\pi$ stacking properties, but in the case of quadruplex DNA, G-tetrads are generally electron-rich and compounds with electron-deficient substituents are considered as good binders (*33*, *39*). However, we observe better quadruplex stabilization here with **EtbzEt** having an ethoxy group compared to its hydroxyl counterpart. It may not be obvious why electron-rich systems have a high affinity for G-tetrads and, in fact, many of the well-known G-quadruplex-stabilizing drugs such as berberine (*51*), telomestatin (*52*), daunomycin (*53*), adriamycin (*54*), etc., where the side groups have overall electron-donating character. In our case, an ethoxy group might provide some kind of stabilization, while in the case of **HyBzEt** and **HyBzMe**, the phenolic OH group may ionize partially to reduce its affinity for DNA. The benzimidazole H atoms might also play some role in the structural transition and consequent stabilization of the G-quadruplex DNA. The hydroxyl of the 2-hydroxyethyl group at the piperazine unit might help in binding with the thymine residues of the loops probably by hydrogen bonding.

In the electrophoresis experiments, both the original quadruplex band and the band emerging after interaction with **EtBzEt** exhibited a mobility higher than that of the T_{20} marker. It is well documented that the intramolecular quadruplex formed by the sequence $d(T_2G_4)_4$ (in K^+ solution) has a mobility corresponding to that of a T_{15} marker (*38*). Hence, our results indicate that the difference in the mobility of the drug−DNA complex is due to the change in the topology of the quadruplex after its interaction with the compound. **EtBzEt** also converts the hybrid intramolecular quadruplex here into a parallel intramolecular quadruplex.

Taken together, the CD titration and electrophoresis data are consistent with the notion that these new compounds are able to convert the antiparallel intramolecular quadruplex into the parallel intramolecular quadruplex, and if it is intermolecular, there is further retardation in the mobility. A similar observation was reported with the human telomeric DNA sequence when the quadruplex was formed in the presence of PEG (*55*). In that work, the authors proposed the conversion from a hybrid structure to a parallel propeller structure.

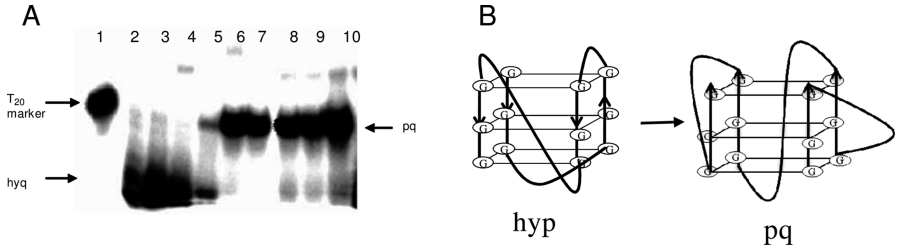

FIGURE 13: (A) Emergence of a new band in the electrophoresis of the $d(T_2G_4)_4$ quadruplex formed in the indicated salt: lane 1, T_{20} marker; lane 2, 5 μM $(T_2G_4)_4$ in 100 mM Li^+ and 10 mM Na^+; lanes 3 and 4, 5 μM quadruplex in 100 mM Na^+; lanes 5−7, 5 μM quadruplex in 100 mM Na^+ with 25, 50, and 65 μM **EtBzEt**, respectively; and lanes 8−10, 5 μM quadruplex in 100 mM Li^+ with 25, 50, and 65 μM **EtBzEt**, respectively. hyq denotes the hybrid intramolecular quadruplex and pq the parallel intramolecular quadruplex. (B) Model for the proposed structural conversion.

In summary, we have synthesized four new compounds having higher affinity for G-quadruplex DNA. Bisbenzimidazole compounds are known for their biological properties (*30*). Substitution of the electron-donating group further increases their cell compatibility and binding affinity (*31*). For the compounds having molecular size comparable to that of the G-quartet, the interference caused by duplex DNA when compounds are injected in vivo might be less significant (*14*, *46*). Our data also suggest that these compounds will have significantly lower affinity for the duplex DNA via either mode of binding [minor groove binding and intercalation (Supporting Information)]. Binding constant data also suggest a much lower affinity of **EtBzEt** toward duplex DNA compared to that of quadruplex DNA (Table 2). These compounds not only stabilize and alter the structure of the preformed *Tetrahymena* G-quadruplex but also induce formation of the quadruplex in the absence of added cations. This observation is particularly interesting. Most notably, these molecules induce parallel-type topologies of quadruplex DNA. The molecular recognition properties of quadruplex DNA will presumably change if its naturally dominant form can be altered in the presence of a ligand. These compounds may also induce certain structural changes in the quadruplex DNA made with human telomeric repeats. In this regard, these compounds may serve as important ligands in improving our understanding of the biology of quadruplex−ligand interactions.

SUPPORTING INFORMATION AVAILABLE

Additional CD titrations, calculations of the gas-phase conformation and effects of solvation, schematic representation of molecular stacking on the G-quartet and interatomic distances in **EtBzEt**, and electrophoresis of the $d(T_2G_4)_4$ quadruplex. This material is available free of charge via the Internet at http://pubs.acs.org.

REFERENCES

1. Blackburn, E. H., and Szostak, J. W. (1984) The molecular structure of centromers and telomers. *Annu. Rev. Biochem. 53*, 163–194.
2. Blackburn, E. H. (1991) Structure and function of telomers. *Nature 350*, 569–573.
3. Davis, J. T. (2004) G-Quartets 40 years later: From 5′-GMP to molecular biology and supramolecular chemistry. *Angew. Chem., Int. Ed. 43*, 668–669.
4. Franceschin, M. (2009) G-Quadruplex DNA structures and organic chemistry: More than one connection. *Eur. J. Org. Chem.,* 2225–2238.
5. Gowan, S. M., Harrison, J. R., Patterson, L., Valneti, M., Read, M. A., Neidle, S., and Kelland, L. R. (2002) A G-quadruplex-interactive potent small-molecule inhibitor of telomerase exhibiting in vitro and in vivo antitumor activity. *Mol. Pharmacol. 61*, 1154–1162.
6. Cech, T. R. (2000) Life at the end of the chromosome: Telomeres and telomerase. *Angew. Chem., Int. Ed. 39*, 34–43.
7. Mergny, J.-L., and Helene, C. (1998) G-Quadruplex DNA: A target for drug design. *Nat. Med. 4*, 1366–1367.
8. Han, H., and Hurley, L. H. (2000) G-Quadruplex DNA: A potential target for anti-cancer drug design. *Trends Pharmacol. Sci. 21*, 136–141.
9. Burger, A. M., Dai, F., Schultes, C. M., Reszka, A. P., Moore, M. J., Double, J. A., and Neidle, S. (2005) The G-quadruplex-interactive molecule BRACO-19 inhibits tumor growth, consistent with telomere targeting and interference with telomerase function. *Cancer Res. 65*, 1489–1496.
10. Moorehouse, A. D., Santos, A. M., Gunaratnam, M., Moore, M., Neidle, S., and Mosses, J. E. (2006) Stabilization of G-quadruplex DNA by highly selective ligands via click chemistry. *J. Am. Chem. Soc. 128*, 15972–15973.
11. Monchaud, D., Yang, P., Lacroix, L., Teulade-Fichou, M.-P., and Mergny, J.-L. (2008) A metal-mediated conformational switch controls G-quadruplex binding affinity. *Angew. Chem., Int. Ed. 47*, 4858–4861.
12. Muller, S., Pantos, G. D., Rodriguez, R., and Balasubramanian, S. (2009) Controlled folding of a small molecule modulates DNA G-quadruplex recognition. *Chem. Commun.,* 80–82.
13. Dash, J., Shirude, P. S., and Balasubramanian, S. (2008) G-Quadruplex recognition by bis-indole carboxamides. *Chem. Commun.,* 3055–3057.
14. Li, G., Huang, J., Zhang, M., Zhou, Y., Zhang, D., Wu, Z., Wang, S., Weng, X., Zhou, X., and Yang, G. (2008) Bis(benzimidazole)pyridine derivative as a new class of G-quadruplex inducing and stabilizing ligand. *Chem. Commun.,* 4564–4566.
15. Rodriguez, R., Pantos, G. D., Goncalves, D. P. N., Sanders, J. K. M., and Balabubramanian, S. (2007) Ligand induced-driven G-quadruplex conformational switching by using an unusual mode of interaction. *Angew. Chem., Int. Ed. 46*, 5405–5407.
16. Bhattacharya, S., and Mandal, S. S. (1995) Ambient oxygen activating water soluble cobalt-salen complex for DNA cleavage. *J. Chem. Soc., Chem. Commun.,* 2489–2490.
17. Bhattacharya, S., and Mandal, S. S. (1996) DNA cleavage by intercalatable cobalt-bispicolylamine complexes activated by visible light. *Chem. Commun.,* 1515–1516.
18. Mandal, S. S., Kumar, N. V., Varshney, U., and Bhattacharya, S. (1996) Metal-ion-dependent oxidative DNA cleavage by transition metal complexes of a new water-soluble salen derivative. *J. Inorg. Biochem. 63*, 265–272.
19. Mandal, S. S., Varshney, U., and Bhattacharya, S. (1997) Role of the central metal ion and ligand charge in the DNA binding and modification by metallosalen complexes. *Bioconjugate Chem. 8*, 798–812.
20. Bhattacharya, S., and Thomas, M. (2000) DNA binding properties of novel distamycin analogs that lack the leading amide unit at the N-terminus. *Biochem. Biophys. Res. Commun. 267*, 139–144.
21. Ghosh, S., Defrancq, E., Lhomme, J. H., Dumy, P., and Bhattacharya, S. (2004) Efficient conjugation and characterization of distamycin-based peptides with selected oligonucleotide stretches. *Bioconjugate Chem. 15*, 520–529.
22. Chaudhuri, P., Majumder, H. K., and Bhattacharya, S. (2007) Synthesis, DNA binding, and *leishmania* topoisomerase inhibition activities of a novel series of anthra [1,2-*d*]imidazole-6,11-dione derivatives. *J. Med. Chem. 50*, 2536–2540.
23. Chaudhuri, P., Ganguly, B., and Bhattacharya, S. (2007) An experimental and computational analysis on the differential role of the

positional isomers of symmetric bis-2-(pyridyl)-1*H*-benzimidazoles as DNA binding agents. *J. Org. Chem. 72*, 1912–1923.
24. Bathini, Y., Rao, K. E., Shea, R. G., and Lown, W. (1990) Molecular recognition between ligands and nucleic acids: Novel pyridine- and benzoxazole-containing agents related to Hoechst 33258 that exhibit altered DNA sequence specificity deduced from footprinting analysis and spectroscopic studies. *Chem. Res. Toxicol. 3*, 268–280.
25. Frisch, M. J., Trucks, G. W., Schlegel, H. B., Scuseria, G. E., Robb, M. A., Cheeseman, J. R., Montgomery, J. A., Vreven, T., Jr., Kudin, K. N., Burant, J. C., Milliam, J. M., et al. (2004) Gaussian 03, Gaussian, Inc., Wallingford, CT.
26. Peacocke, A. R., and Skerrett, J. N. H. (1956) The interaction of amino-acridines with nucleic acids. *J. Chem. Soc., Faraday Trans. 52*, 261–279.
27. Stokke, T., and Steen, H. B. (1985) Multiple binding modes for Hoechst 33258 to DNA. *J. Histochem. Cytochem. 33*, 333–338.
28. Holmquist, G. (1975) Hoechst 33258 fluorescent staining of *drosophila* chromosomes. *Chromosoma 49*, 333–356.
29. Latt, S. A., and Wohlleb, J. C. (1975) Optical studies of the interaction of 33258 Hoechst with DNA, chromatin, and metaphase chromosomes. *Chromosoma 52*, 297–316.
30. Bhattacharya, S., and Chaudhuri, P. (2008) Medical implications of benzimidazole derivatives as drugs designed for targeting DNA and DNA associated processes. *Curr. Med. Chem. 15*, 1762–1777.
31. Tawar, U., Jain, A. K., Dwarakanath, B. S., Chandra, R., Singh, Y., Chaudhury, N. K., Khaitan, D., and Tandon, V. (2003) Influence of phenyl ring disubstitution on bisbenzimidazole and terbenzimidazole cytotoxicity: Synthesis and biological evaluation as radioprotectors. *J. Med. Chem. 46*, 3785–3792.
32. Hori, Y., Bichenkova, E. V., Wilton, A. N., El-Attug, M. N., Sadat-Ebrahimi, S., Tanaka, T., Kikuchi, Y., Araki, M., Sugiura, Y., and Douglas, K. T. (2001) Synthetic inhibitors of the processing of pretransfer RNA by the ribonuclease P ribozyme: Enzyme inhibitors which act by binding to substrate. *Biochemistry 40*, 603–608.
33. Kieltyka, R., Fakhoury, J., Moitessier, N., and Sleiman, H. F. (2008) Platinum phenanthroimidazole complexes as G-quadruplex DNA selective binders. *Chem.—Eur. J. 14*, 1145–1154.
34. Arora, A., Balasubramanian, C., Kumar, N., Agrawal, S., Ojha, R. P., and Maiti, S. (2008) Binding of berberine to human telomeric quadruplex: Spectroscopic, calorimetric and molecular modeling studies. *FEBS J. 275*, 3971–3983.
35. Parkinson, G. N., Lee, M. P. H., and Neidle, S. (2002) Crystal structure of parallel quadruplexs from human telomeric DNA. *Nature 417*, 876–880.
36. Hardin, C. C., Henderson, E., Watson, T., and Prosser, J. K. (1991) Monovalent cation induced structural transitions in telomeric DNAs: G-DNA folding intermediates. *Biochemistry 30*, 4460–4472.
37. Chen, F.-M. (1992) Sr^{2+} facilitates intermolecular G-quadruplex formation of telomeric sequences. *Biochemistry 31*, 3769–3776.
38. Oganesian, L., Moon, I. K., Bryan, T. M., and Jarstfer, M. B. (2006) Extension of G-quadruplex DNA by ciliate telomerase. *EMBO J. 25*, 1148–1159.
39. Murashima, T., Sakiyama, D., Miyoshi, D., Kuriyama, M., Yamada, T., Miyazawa, T., and Sugimoto, N. (2009) Cationic porphyrin induced a telomeric DNA to G-quadruplex form in water. *Bioinorg. Chem. Appl.* DOI 10.1155/2008/294756.
40. Martino, L., Virno, A., Pagano, B., Virgillo, A., Di Micco, S., Galeone, A., Giancola, C., Bifulco, G., Mayo, L., and Randazzo, A. (2007) Structural and thermodynamic studies of the interaction of distamycin A with the parallel quadruplex structure. *J. Am. Chem. Soc. 129*, 16048–16056.
41. Wang, Y., and Patel, D. J. (1994) Solution structure of the *Tetrahymena* telomeric repeat $d(T_2G_4)_4$ G-tetraplex. *Structure 2*, 1141–1156.
42. Dapic, V., Abdomerovic, V., Marrington, R., Peberdy, J., Rodger, A., Trent, J. O., and Bates, P. J. (2003) Biophysical and biological properties of quadruplex oligodeoxyribonucleotides. *Nucleic Acids Res. 31*, 2097–2107.
43. Cian, A., Guittat, L., Kaiser, M., Sacca, B., Amrane, S., Bourdoncle, A., Albertti, P., Teulade-Fichou, M.-P., Lacriox, L., and Mergny, J.-L. (2007) Fluorescence-based melting assays for studying quadruplex ligands. *Methods 42*, 183–195.
44. Diana, P. N., Gonçalves, R. R., Balasubramanian, S., and Sander, J. K. M. (2006) Tetramethylpyridinium phorphyrazines: A new class of G-quadruplex inducing and stabilising ligands. *Chem. Commun.,* 4685–4687.
45. Yang, D.-Y., Chang, T.-C., and Sheu, S.-Y. (2007) Interaction between human telomere and a carbazole derivative: A molecular dynamics simulation of a quadruplex stabilizer and telomerase inhibitor. *J. Phys. Chem. A 111*, 9224–9232.
46. Campbell, N. H., Parkinson, G. N., Reszka, A. P., and Neidle, S. (2008) Structural basis of DNA quadruplex recognition by an acridine drug. *J. Am. Chem. Soc. 130*, 6722–6724.
47. Redman, J. E., Granadino-Roldan, J. M., Schouten, J. A., Ladame, S., Reszka, A. P., Neidle, S., and Balasubramanian, S. (2009) Recognition and discrimination of DNA quadruplexes by acridine-peptide conjugates. *Org. Biomol. Chem. 7*, 76–84.
48. Kaushik, M., and Kukreti, S. (2003) Temperature induced hyperchromism exhibited by Hoechst 33258: Evidence of drug aggregation from UV-melting method. *Spectrochim. Acta, Part A 59*, 3123–3129.
49. Kobayashi, M., Kusakawa, T., Saito, M., Kaji, S., Oomura, S., Morita, Y., Hasan, Q., and Tamiya, E. (2004) Electrochemical DNA quantification based on aggregation induced by Hoechst 33258. *Electrochem. Commun. 6*, 337–243.
50. Qian, X., Tao, Z.-F., Wei, D., and Sun, J. (1996) Synthesis, crystal structure, and properties of 2H-4,8-dimethylfuro[2′,3′:5,6]naphtho-[1,2-b]pyran-2-one, a novel DNA intercalator. *Monatsh. Chem. 127*, 569–577.
51. Franceschin, M., Rossetti, L., Ambrosio, A. D., Schirripa, S., Bianco, A., Ortaggi, G., Savino, M., Schults, C., and Neidle, S. (2006) Natural and synthetic G-quadruplex interactive berberine derivatives. *Bioorg. Med. Chem. Lett. 16*, 1707–1711.
52. Gomez, D., Paterski, R., Lemarteleur, T., Shin-ya, K., Mergny, J.-L., and Riou, J.-F. (2004) Interaction of telomestatin with telomeric single-strand overhang. *J. Biol. Chem. 279*, 41487–41494.
53. Clark, G. R., Pytel, P. D., Squire, C. I., and Neidle, S. (2003) Structure of first parallel DNA quadruplex-drug complex. *J. Am. Chem. Soc. 125*, 4066–4067.
54. Huang, H.-S., Chon, C.-L., Guo, C.-L., Yuan, C.-L., Lu, Y.-C., Shieh, F.-Y., and Liu, J.-J. (2005) Human telomeric inhibition and cytotoxity of regioisomeric disubstituted amidoanthraquinones and aminoanthraquinones. *Bioorg. Med. Chem. 13*, 1435–1444.
55. Xue, Y., Kan, Z.-Y., Wang, Q., Yao, Y., Liu, J., Hao, Y.-H., and Tan, Z. (2007) Human telomeric DNA forms parallel-stranded intramolecular G-quadruplex in K^+ solution under molecular crowding condition. *J. Am. Chem. Soc. 129*, 11185–11191.